BABAR-PUB-06/035
SLAC-PUB-11923
hep-ex/0606054
June 2006

Observation of e^+e^- Annihilations into the $C = +1$ Hadronic Final States $\rho^0\rho^0$ and $\phi\rho^0$

B. Aubert,[1] R. Barate,[1] M. Bona,[1] D. Boutigny,[1] F. Couderc,[1] Y. Karyotakis,[1] J. P. Lees,[1] V. Poireau,[1]
V. Tisserand,[1] A. Zghiche,[1] E. Grauges,[2] A. Palano,[3] J. C. Chen,[4] N. D. Qi,[4] G. Rong,[4] P. Wang,[4] Y. S. Zhu,[4]
G. Eigen,[5] I. Ofte,[5] B. Stugu,[5] G. S. Abrams,[6] M. Battaglia,[6] D. N. Brown,[6] J. Button-Shafer,[6] R. N. Cahn,[6]
E. Charles,[6] M. S. Gill,[6] Y. Groysman,[6] R. G. Jacobsen,[6] J. A. Kadyk,[6] L. T. Kerth,[6] Yu. G. Kolomensky,[6]
G. Kukartsev,[6] G. Lynch,[6] L. M. Mir,[6] P. J. Oddone,[6] T. J. Orimoto,[6] M. Pripstein,[6] N. A. Roe,[6] M. T. Ronan,[6]
W. A. Wenzel,[6] P. del Amo Sanchez,[7] M. Barrett,[7] K. E. Ford,[7] T. J. Harrison,[7] A. J. Hart,[7] C. M. Hawkes,[7]
S. E. Morgan,[7] A. T. Watson,[7] K. Goetzen,[8] T. Held,[8] H. Koch,[8] B. Lewandowski,[8] M. Pelizaeus,[8] K. Peters,[8]
T. Schroeder,[8] M. Steinke,[8] J. T. Boyd,[9] J. P. Burke,[9] W. N. Cottingham,[9] D. Walker,[9] T. Cuhadar-Donszelmann,[10]
B. G. Fulsom,[10] C. Hearty,[10] N. S. Knecht,[10] T. S. Mattison,[10] J. A. McKenna,[10] A. Khan,[11] P. Kyberd,[11]
M. Saleem,[11] D. J. Sherwood,[11] L. Teodorescu,[11] V. E. Blinov,[12] A. D. Bukin,[12] V. P. Druzhinin,[12]
V. B. Golubev,[12] A. P. Onuchin,[12] S. I. Serednyakov,[12] Yu. I. Skovpen,[12] E. P. Solodov,[12] K. Yu Todyshev,[12]
D. S. Best,[13] M. Bondioli,[13] M. Bruinsma,[13] M. Chao,[13] S. Curry,[13] I. Eschrich,[13] D. Kirkby,[13] A. J. Lankford,[13]
P. Lund,[13] M. Mandelkern,[13] R. K. Mommsen,[13] W. Roethel,[13] D. P. Stoker,[13] S. Abachi,[14] C. Buchanan,[14]
S. D. Foulkes,[15] J. W. Gary,[15] O. Long,[15] B. C. Shen,[15] K. Wang,[15] L. Zhang,[15] H. K. Hadavand,[16] E. J. Hill,[16]
H. P. Paar,[16] S. Rahatlou,[16] V. Sharma,[16] J. W. Berryhill,[17] C. Campagnari,[17] A. Cunha,[17] B. Dahmes,[17]
T. M. Hong,[17] D. Kovalskyi,[17] J. D. Richman,[17] T. W. Beck,[18] A. M. Eisner,[18] C. J. Flacco,[18] C. A. Heusch,[18]
J. Kroseberg,[18] W. S. Lockman,[18] G. Nesom,[18] T. Schalk,[18] B. A. Schumm,[18] A. Seiden,[18] P. Spradlin,[18]
D. C. Williams,[18] M. G. Wilson,[18] J. Albert,[19] E. Chen,[19] A. Dvoretskii,[19] F. Fang,[19] D. G. Hitlin,[19] I. Narsky,[19]
T. Piatenko,[19] F. C. Porter,[19] A. Ryd,[19] A. Samuel,[19] G. Mancinelli,[20] B. T. Meadows,[20] M. D. Sokoloff,[20]
F. Blanc,[21] P. C. Bloom,[21] S. Chen,[21] W. T. Ford,[21] J. F. Hirschauer,[21] A. Kreisel,[21] U. Nauenberg,[21] A. Olivas,[21]
W. O. Ruddick,[21] J. G. Smith,[21] K. A. Ulmer,[21] S. R. Wagner,[21] J. Zhang,[21] A. Chen,[22] E. A. Eckhart,[22]
A. Soffer,[22] W. H. Toki,[22] R. J. Wilson,[22] F. Winklmeier,[22] Q. Zeng,[22] D. D. Altenburg,[23] E. Feltresi,[23]
A. Hauke,[23] H. Jasper,[23] A. Petzold,[23] B. Spaan,[23] T. Brandt,[24] V. Klose,[24] H. M. Lacker,[24] W. F. Mader,[24]
R. Nogowski,[24] J. Schubert,[24] K. R. Schubert,[24] R. Schwierz,[24] J. E. Sundermann,[24] A. Volk,[24] D. Bernard,[25]
G. R. Bonneaud,[25] P. Grenier,[25,*] E. Latour,[25] Ch. Thiebaux,[25] M. Verderi,[25] D. J. Bard,[26] P. J. Clark,[26]
W. Gradl,[26] F. Muheim,[26] S. Playfer,[26] A. I. Robertson,[26] Y. Xie,[26] M. Andreotti,[27] D. Bettoni,[27] C. Bozzi,[27]
R. Calabrese,[27] G. Cibinetto,[27] E. Luppi,[27] M. Negrini,[27] A. Petrella,[27] L. Piemontese,[27] E. Prencipe,[27]
F. Anulli,[28] R. Baldini-Ferroli,[28] A. Calcaterra,[28] R. de Sangro,[28] G. Finocchiaro,[28] S. Pacetti,[28] P. Patteri,[28]
I. M. Peruzzi,[28,†] M. Piccolo,[28] M. Rama,[28] A. Zallo,[28] A. Buzzo,[29] R. Capra,[29] R. Contri,[29] M. Lo Vetere,[29]
M. M. Macri,[29] M. R. Monge,[29] S. Passaggio,[29] C. Patrignani,[29] E. Robutti,[29] A. Santroni,[29] S. Tosi,[29]
G. Brandenburg,[30] K. S. Chaisanguanthum,[30] M. Morii,[30] J. Wu,[30] R. S. Dubitzky,[31] J. Marks,[31] S. Schenk,[31]
U. Uwer,[31] W. Bhimji,[32] D. A. Bowerman,[32] P. D. Dauncey,[32] U. Egede,[32] R. L. Flack,[32] J .A. Nash,[32]
M. B. Nikolich,[32] W. Panduro Vazquez,[32] X. Chai,[33] M. J. Charles,[33] U. Mallik,[33] N. T. Meyer,[33] V. Ziegler,[33]
J. Cochran,[34] H. B. Crawley,[34] L. Dong,[34] V. Eyges,[34] W. T. Meyer,[34] S. Prell,[34] E. I. Rosenberg,[34] A. E. Rubin,[34]
A. V. Gritsan,[35] M. Fritsch,[36] G. Schott,[36] N. Arnaud,[37] M. Davier,[37] G. Grosdidier,[37] A. Höcker,[37] F. Le
Diberder,[37] V. Lepeltier,[37] A. M. Lutz,[37] A. Oyanguren,[37] S. Pruvot,[37] S. Rodier,[37] P. Roudeau,[37] M. H. Schune,[37]
A. Stocchi,[37] W. F. Wang,[37] G. Wormser,[37] C. H. Cheng,[38] D. J. Lange,[38] D. M. Wright,[38] C. A. Chavez,[39]
I. J. Forster,[39] J. R. Fry,[39] E. Gabathuler,[39] R. Gamet,[39] K. A. George,[39] D. E. Hutchcroft,[39] D. J. Payne,[39]
K. C. Schofield,[39] C. Touramanis,[39] A. J. Bevan,[40] F. Di Lodovico,[40] W. Menges,[40] R. Sacco,[40] G. Cowan,[41]
H. U. Flaecher,[41] D. A. Hopkins,[41] P. S. Jackson,[41] T. R. McMahon,[41] S. Ricciardi,[41] F. Salvatore,[41] A. C. Wren,[41]
D. N. Brown,[42] C. L. Davis,[42] J. Allison,[43] N. R. Barlow,[43] R. J. Barlow,[43] Y. M. Chia,[43] C. L. Edgar,[43]
G. D. Lafferty,[43] M. T. Naisbit,[43] J. C. Williams,[43] J. I. Yi,[43] C. Chen,[44] W. D. Hulsbergen,[44] A. Jawahery,[44]
C. K. Lae,[44] D. A. Roberts,[44] G. Simi,[44] G. Blaylock,[45] C. Dallapiccola,[45] S. S. Hertzbach,[45] X. Li,[45]
T. B. Moore,[45] S. Saremi,[45] H. Staengle,[45] R. Cowan,[46] G. Sciolla,[46] S. J. Sekula,[46] M. Spitznagel,[46] F. Taylor,[46]

Submitted to Physical Review Letters

Work supported in part by Department of Energy contract DE-AC02-76SF00515

R. K. Yamamoto,[46] H. Kim,[47] P. M. Patel,[47] S. H. Robertson,[47] A. Lazzaro,[48] V. Lombardo,[48] F. Palombo,[48] J. M. Bauer,[49] L. Cremaldi,[49] V. Eschenburg,[49] R. Godang,[49] R. Kroeger,[49] D. A. Sanders,[49] D. J. Summers,[49] H. W. Zhao,[49] S. Brunet,[50] D. Côté,[50] P. Taras,[50] F. B. Viaud,[50] H. Nicholson,[51] N. Cavallo,[52, ‡] G. De Nardo,[52] F. Fabozzi,[52, ‡] C. Gatto,[52] L. Lista,[52] D. Monorchio,[52] P. Paolucci,[52] D. Piccolo,[52] C. Sciacca,[52] M. Baak,[53] G. Raven,[53] H. L. Snoek,[53] C. P. Jessop,[54] J. M. LoSecco,[54] T. Allmendinger,[55] G. Benelli,[55] K. K. Gan,[55] K. Honscheid,[55] D. Hufnagel,[55] P. D. Jackson,[55] H. Kagan,[55] R. Kass,[55] A. M. Rahimi,[55] R. Ter-Antonyan,[55] Q. K. Wong,[55] N. L. Blount,[56] J. Brau,[56] R. Frey,[56] O. Igonkina,[56] M. Lu,[56] C. T. Potter,[56] R. Rahmat,[56] N. B. Sinev,[56] D. Strom,[56] J. Strube,[56] E. Torrence,[56] F. Galeazzi,[57] A. Gaz,[57] M. Margoni,[57] M. Morandin,[57] A. Pompili,[57] M. Posocco,[57] M. Rotondo,[57] F. Simonetto,[57] R. Stroili,[57] C. Voci,[57] M. Benayoun,[58] J. Chauveau,[58] P. David,[58] L. Del Buono,[58] Ch. de la Vaissière,[58] O. Hamon,[58] B. L. Hartfiel,[58] M. J. J. John,[58] J. Malclès,[58] J. Ocariz,[58] L. Roos,[58] G. Therin,[58] P. K. Behera,[59] L. Gladney,[59] J. Panetta,[59] M. Biasini,[60] R. Covarelli,[60] C. Angelini,[61] G. Batignani,[61] S. Bettarini,[61] F. Bucci,[61] G. Calderini,[61] M. Carpinelli,[61] R. Cenci,[61] F. Forti,[61] M. A. Giorgi,[61] A. Lusiani,[61] G. Marchiori,[61] M. A. Mazur,[61] M. Morganti,[61] N. Neri,[61] G. Rizzo,[61] J. J. Walsh,[61] M. Haire,[62] D. Judd,[62] D. E. Wagoner,[62] J. Biesiada,[63] N. Danielson,[63] P. Elmer,[63] Y. P. Lau,[63] C. Lu,[63] J. Olsen,[63] A. J. S. Smith,[63] A. V. Telnov,[63] F. Bellini,[64] G. Cavoto,[64] A. D'Orazio,[64] D. del Re,[64] E. Di Marco,[64] R. Faccini,[64] F. Ferrarotto,[64] F. Ferroni,[64] M. Gaspero,[64] L. Li Gioi,[64] M. A. Mazzoni,[64] S. Morganti,[64] G. Piredda,[64] F. Polci,[64] F. Safai Tehrani,[64] C. Voena,[64] M. Ebert,[65] H. Schröder,[65] R. Waldi,[65] T. Adye,[66] N. De Groot,[66] B. Franek,[66] E. O. Olaiya,[66] F. F. Wilson,[66] S. Emery,[67] A. Gaidot,[67] S. F. Ganzhur,[67] G. Hamel de Monchenault,[67] W. Kozanecki,[67] M. Legendre,[67] G. Vasseur,[67] Ch. Yèche,[67] M. Zito,[67] X. R. Chen,[68] H. Liu,[68] W. Park,[68] M. V. Purohit,[68] J. R. Wilson,[68] M. T. Allen,[69] D. Aston,[69] R. Bartoldus,[69] P. Bechtle,[69] N. Berger,[69] R. Claus,[69] J. P. Coleman,[69] M. R. Convery,[69] M. Cristinziani,[69] J. C. Dingfelder,[69] J. Dorfan,[69] G. P. Dubois-Felsmann,[69] D. Dujmic,[69] W. Dunwoodie,[69] R. C. Field,[69] T. Glanzman,[69] S. J. Gowdy,[69] M. T. Graham,[69] V. Halyo,[69] C. Hast,[69] T. Hryn'ova,[69] W. R. Innes,[69] M. H. Kelsey,[69] P. Kim,[69] D. W. G. S. Leith,[69] S. Li,[69] S. Luitz,[69] V. Luth,[69] H. L. Lynch,[69] D. B. MacFarlane,[69] H. Marsiske,[69] R. Messner,[69] D. R. Muller,[69] C. P. O'Grady,[69] V. E. Ozcan,[69] A. Perazzo,[69] M. Perl,[69] T. Pulliam,[69] B. N. Ratcliff,[69] A. Roodman,[69] A. A. Salnikov,[69] R. H. Schindler,[69] J. Schwiening,[69] A. Snyder,[69] J. Stelzer,[69] D. Su,[69] M. K. Sullivan,[69] K. Suzuki,[69] S. K. Swain,[69] J. M. Thompson,[69] J. Va'vra,[69] N. van Bakel,[69] M. Weaver,[69] A. J. R. Weinstein,[69] W. J. Wisniewski,[69] M. Wittgen,[69] D. H. Wright,[69] A. K. Yarritu,[69] K. Yi,[69] C. C. Young,[69] P. R. Burchat,[70] A. J. Edwards,[70] S. A. Majewski,[70] B. A. Petersen,[70] C. Roat,[70] L. Wilden,[70] S. Ahmed,[71] M. S. Alam,[71] R. Bula,[71] J. A. Ernst,[71] V. Jain,[71] B. Pan,[71] M. A. Saeed,[71] F. R. Wappler,[71] S. B. Zain,[71] W. Bugg,[72] M. Krishnamurthy,[72] S. M. Spanier,[72] R. Eckmann,[73] J. L. Ritchie,[73] A. Satpathy,[73] C. J. Schilling,[73] R. F. Schwitters,[73] J. M. Izen,[74] X. C. Lou,[74] S. Ye,[74] F. Bianchi,[75] F. Gallo,[75] D. Gamba,[75] M. Bomben,[76] L. Bosisio,[76] C. Cartaro,[76] F. Cossutti,[76] G. Della Ricca,[76] S. Dittongo,[76] L. Lanceri,[76] L. Vitale,[76] V. Azzolini,[77] F. Martinez-Vidal,[77] Sw. Banerjee,[78] B. Bhuyan,[78] C. M. Brown,[78] D. Fortin,[78] K. Hamano,[78] R. Kowalewski,[78] I. M. Nugent,[78] J. M. Roney,[78] R. J. Sobie,[78] J. J. Back,[79] P. F. Harrison,[79] T. E. Latham,[79] G. B. Mohanty,[79] M. Pappagallo,[79] H. R. Band,[80] X. Chen,[80] B. Cheng,[80] S. Dasu,[80] M. Datta,[80] K. T. Flood,[80] J. J. Hollar,[80] P. E. Kutter,[80] B. Mellado,[80] A. Mihalyi,[80] Y. Pan,[80] M. Pierini,[80] R. Prepost,[80] S. L. Wu,[80] Z. Yu,[80] and H. Neal[81]

(The *BABAR* Collaboration)

[1]*Laboratoire de Physique des Particules, F-74941 Annecy-le-Vieux, France*
[2]*Universitat de Barcelona, Facultat de Fisica Dept. ECM, E-08028 Barcelona, Spain*
[3]*Università di Bari, Dipartimento di Fisica and INFN, I-70126 Bari, Italy*
[4]*Institute of High Energy Physics, Beijing 100039, China*
[5]*University of Bergen, Institute of Physics, N-5007 Bergen, Norway*
[6]*Lawrence Berkeley National Laboratory and University of California, Berkeley, California 94720, USA*
[7]*University of Birmingham, Birmingham, B15 2TT, United Kingdom*
[8]*Ruhr Universität Bochum, Institut für Experimentalphysik 1, D-44780 Bochum, Germany*
[9]*University of Bristol, Bristol BS8 1TL, United Kingdom*
[10]*University of British Columbia, Vancouver, British Columbia, Canada V6T 1Z1*
[11]*Brunel University, Uxbridge, Middlesex UB8 3PH, United Kingdom*
[12]*Budker Institute of Nuclear Physics, Novosibirsk 630090, Russia*
[13]*University of California at Irvine, Irvine, California 92697, USA*
[14]*University of California at Los Angeles, Los Angeles, California 90024, USA*
[15]*University of California at Riverside, Riverside, California 92521, USA*
[16]*University of California at San Diego, La Jolla, California 92093, USA*

[17]*University of California at Santa Barbara, Santa Barbara, California 93106, USA*
[18]*University of California at Santa Cruz, Institute for Particle Physics, Santa Cruz, California 95064, USA*
[19]*California Institute of Technology, Pasadena, California 91125, USA*
[20]*University of Cincinnati, Cincinnati, Ohio 45221, USA*
[21]*University of Colorado, Boulder, Colorado 80309, USA*
[22]*Colorado State University, Fort Collins, Colorado 80523, USA*
[23]*Universität Dortmund, Institut für Physik, D-44221 Dortmund, Germany*
[24]*Technische Universität Dresden, Institut für Kern- und Teilchenphysik, D-01062 Dresden, Germany*
[25]*Ecole Polytechnique, Laboratoire Leprince-Ringuet, F-91128 Palaiseau, France*
[26]*University of Edinburgh, Edinburgh EH9 3JZ, United Kingdom*
[27]*Università di Ferrara, Dipartimento di Fisica and INFN, I-44100 Ferrara, Italy*
[28]*Laboratori Nazionali di Frascati dell'INFN, I-00044 Frascati, Italy*
[29]*Università di Genova, Dipartimento di Fisica and INFN, I-16146 Genova, Italy*
[30]*Harvard University, Cambridge, Massachusetts 02138, USA*
[31]*Universität Heidelberg, Physikalisches Institut, Philosophenweg 12, D-69120 Heidelberg, Germany*
[32]*Imperial College London, London, SW7 2AZ, United Kingdom*
[33]*University of Iowa, Iowa City, Iowa 52242, USA*
[34]*Iowa State University, Ames, Iowa 50011-3160, USA*
[35]*Johns Hopkins University, Baltimore, Maryland 21218, USA*
[36]*Universität Karlsruhe, Institut für Experimentelle Kernphysik, D-76021 Karlsruhe, Germany*
[37]*Laboratoire de l'Accélérateur Linéaire, IN2P3-CNRS et Université Paris-Sud 11,*
Centre Scientifique d'Orsay, B.P. 34, F-91898 ORSAY Cedex, France
[38]*Lawrence Livermore National Laboratory, Livermore, California 94550, USA*
[39]*University of Liverpool, Liverpool L69 7ZE, United Kingdom*
[40]*Queen Mary, University of London, E1 4NS, United Kingdom*
[41]*University of London, Royal Holloway and Bedford New College, Egham, Surrey TW20 0EX, United Kingdom*
[42]*University of Louisville, Louisville, Kentucky 40292, USA*
[43]*University of Manchester, Manchester M13 9PL, United Kingdom*
[44]*University of Maryland, College Park, Maryland 20742, USA*
[45]*University of Massachusetts, Amherst, Massachusetts 01003, USA*
[46]*Massachusetts Institute of Technology, Laboratory for Nuclear Science, Cambridge, Massachusetts 02139, USA*
[47]*McGill University, Montréal, Québec, Canada H3A 2T8*
[48]*Università di Milano, Dipartimento di Fisica and INFN, I-20133 Milano, Italy*
[49]*University of Mississippi, University, Mississippi 38677, USA*
[50]*Université de Montréal, Physique des Particules, Montréal, Québec, Canada H3C 3J7*
[51]*Mount Holyoke College, South Hadley, Massachusetts 01075, USA*
[52]*Università di Napoli Federico II, Dipartimento di Scienze Fisiche and INFN, I-80126, Napoli, Italy*
[53]*NIKHEF, National Institute for Nuclear Physics and High Energy Physics, NL-1009 DB Amsterdam, The Netherlands*
[54]*University of Notre Dame, Notre Dame, Indiana 46556, USA*
[55]*Ohio State University, Columbus, Ohio 43210, USA*
[56]*University of Oregon, Eugene, Oregon 97403, USA*
[57]*Università di Padova, Dipartimento di Fisica and INFN, I-35131 Padova, Italy*
[58]*Universités Paris VI et VII, Laboratoire de Physique Nucléaire et de Hautes Energies, F-75252 Paris, France*
[59]*University of Pennsylvania, Philadelphia, Pennsylvania 19104, USA*
[60]*Università di Perugia, Dipartimento di Fisica and INFN, I-06100 Perugia, Italy*
[61]*Università di Pisa, Dipartimento di Fisica, Scuola Normale Superiore and INFN, I-56127 Pisa, Italy*
[62]*Prairie View A&M University, Prairie View, Texas 77446, USA*
[63]*Princeton University, Princeton, New Jersey 08544, USA*
[64]*Università di Roma La Sapienza, Dipartimento di Fisica and INFN, I-00185 Roma, Italy*
[65]*Universität Rostock, D-18051 Rostock, Germany*
[66]*Rutherford Appleton Laboratory, Chilton, Didcot, Oxon, OX11 0QX, United Kingdom*
[67]*DSM/Dapnia, CEA/Saclay, F-91191 Gif-sur-Yvette, France*
[68]*University of South Carolina, Columbia, South Carolina 29208, USA*
[69]*Stanford Linear Accelerator Center, Stanford, California 94309, USA*
[70]*Stanford University, Stanford, California 94305-4060, USA*
[71]*State University of New York, Albany, New York 12222, USA*
[72]*University of Tennessee, Knoxville, Tennessee 37996, USA*
[73]*University of Texas at Austin, Austin, Texas 78712, USA*
[74]*University of Texas at Dallas, Richardson, Texas 75083, USA*
[75]*Università di Torino, Dipartimento di Fisica Sperimentale and INFN, I-10125 Torino, Italy*
[76]*Università di Trieste, Dipartimento di Fisica and INFN, I-34127 Trieste, Italy*
[77]*IFIC, Universitat de Valencia-CSIC, E-46071 Valencia, Spain*
[78]*University of Victoria, Victoria, British Columbia, Canada V8W 3P6*
[79]*Department of Physics, University of Warwick, Coventry CV4 7AL, United Kingdom*

[80]*University of Wisconsin, Madison, Wisconsin 53706, USA*
[81]*Yale University, New Haven, Connecticut 06511, USA*

(Dated: June 23, 2006)

We report the first observation of e^+e^- annihilations into states of positive C-parity, namely $\rho^0\rho^0$ and $\phi\rho^0$. The two states are observed in the $\pi^+\pi^-\pi^+\pi^-$ and $K^+K^-\pi^+\pi^-$ final states, respectively, in a data sample of 225 fb^{-1} collected by the *BABAR* experiment at the PEP-II e^+e^- storage rings at energies near $\sqrt{s} = 10.58$ GeV. The distributions of $\cos\theta^*$, where θ^* is the center-of-mass polar angle of the ϕ meson or the forward ρ^0 meson, suggest production by two-virtual-photon annihilation. We measure cross sections within the range $|\cos\theta^*| < 0.8$ of $\sigma(e^+e^-\to\rho^0\rho^0) = 20.7 \pm 0.7(\text{stat}) \pm 2.7(\text{syst})$ fb and $\sigma(e^+e^-\to\phi\rho^0) = 5.7 \pm 0.5(\text{stat}) \pm 0.8(\text{syst})$ fb.

PACS numbers: 12.20.-m, 12.38.Aw, 12.40.Vv

The process $e^+e^- \to$ hadrons at center-of-mass (CM) energy $\sqrt{s}$ far below the Z^0 mass is dominated by annihilation via a single virtual photon with charge-conjugation parity $C = -1$. The high luminosity of the B factories provides an opportunity to explore rare, low multiplicity final states with $C = +1$ such as those produced in the two-virtual-photon annihilation (TVPA) process depicted in Fig. 1. The TVPA process has been ignored in the interpretation of the total hadronic cross section in e^+e^- annihilations as input to calculations [1] of the muon g–2 and the running QED coupling α. We report the first observation of the exclusive reactions $e^+e^-\to\rho^0\rho^0$ and $e^+e^-\to\phi\rho^0$, in which the final states are even under charge conjugation, and therefore cannot be produced via single-photon annihilation.

This analysis uses a 205 fb^{-1} data sample of e^+e^- collisions collected on the $\Upsilon(4S)$ resonance and 20 fb^{-1} collected 40 MeV below with the *BABAR* detector at the SLAC PEP-II asymmetric-energy B factory. The *BABAR* detector is described in detail elsewhere [2]. Charged-particle momenta and energy loss are measured in the tracking system which consists of a silicon vertex tracker (SVT) and a drift chamber (DCH). Electrons and photons are detected in a CsI(Tl) calorimeter (EMC). An internally reflecting ring-imaging Cherenkov detector (DIRC) provides charged particle identification (PID). An instrumented magnetic flux return (IFR) provides identification of muons. Kaon and pion candidates are identified using likelihoods of particle hypotheses calculated from the specific ionization in the DCH and SVT, and the Cherenkov angle measured in the DIRC. Electrons are identified by the ratio of the energy deposited in the EMC to the momentum and by the shower shape; muons are identified by the depth of penetration into the IFR.

Events with four well-reconstructed charged tracks and a total charge of zero are selected. Charged tracks are required to have at least 12 DCH hits and a polar angle in the range $0.41 < \theta < 2.54$ radians. The momenta of kaon and pion candidates are required to be greater than 800 and 600 MeV/c, respectively. Among the four selected tracks, two oppositely charged tracks must be identified as pions, and the other pair must be identified as two pions or two kaons. Events in which one or more pion candidates are identified as an electron or muon are rejected (lepton veto). We fit the four tracks to a common vertex, and require the χ^2 probability to exceed 0.1%. We accept events with reconstructed invariant mass within 170 MeV/c^2 of the nominal CM energy (Fig. 2).

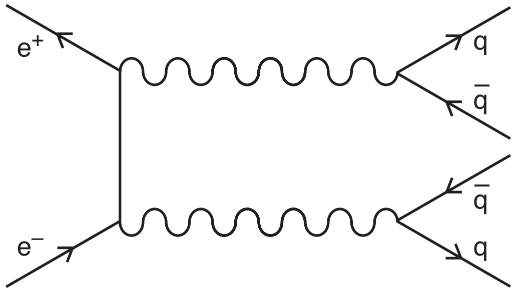

FIG. 1: Two-virtual-photon annihilation diagram.

In the process $e^+e^- \to \pi^+\pi^-\pi^+\pi^-$, there are two possible pairings of π^+ mesons with π^- mesons. However, only one combination appears in the kinematic region of interest ($m_{\pi^+\pi^-} < 2$ GeV/c^2) for both pairs. We label the pion pair with CM momentum vector pointing into the hemisphere defined by the e^- beam direction $\pi^+\pi^-_f$ and the other as $\pi^+\pi^-_b$. Figure 3(a) shows the scatter plot of the invariant masses of $\pi^+\pi^-_f$ and $\pi^+\pi^-_b$ from $e^+e^- \to \pi^+\pi^-\pi^+\pi^-$ events, and Fig. 3(b) the plot of invariant masses of K^+K^- and $\pi^+\pi^-$ pairs from $e^+e^- \to K^+K^-\pi^+\pi^-$ events. We observe correlations of masses in Fig. 3(a) indicating the production of $\rho^0\rho^0$ final states, and in Fig. 3(b) indicating the production of $\phi\rho^0$ final states.

To extract the number of $e^+e^- \to \rho^0\rho^0$ and $\phi\rho^0$ signal events, we perform a binned maximum-likelihood fit for nine rectangular regions (tiles) in the two-dimensional mass distributions, as shown in Fig. 3. The signal box is the central tile (tile 5), defined by the mass ranges $0.5 < m_{\pi^+\pi^-} < 1.1$ GeV/c^2 and $1.008 < m_{K^+K^-} < 1.035$ GeV/c^2. For $e^+e^- \to K^+K^-\pi^+\pi^-$, the expected number of events, n_i, for each tile i can be expressed as:

$$n_i = f_i^S S + f_i^\phi N_\phi + f_i^{\rho^0} N_{\rho^0} + f_i^B B, \qquad (1)$$

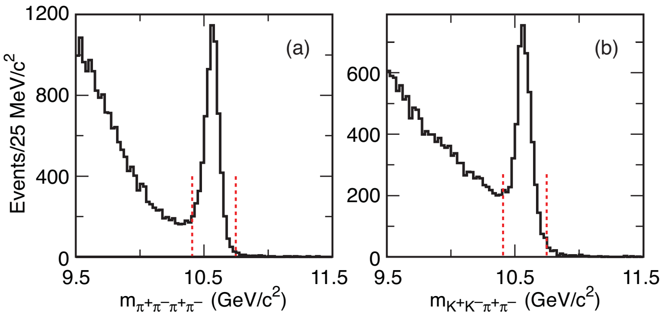

FIG. 2: Distributions of the invariant mass ($\Upsilon(4S)$ data) for the a) $\pi^+\pi^-\pi^+\pi^-$ and b) $K^+K^-\pi^+\pi^-$ final states. The accepted signal regions are indicated by the dashed lines.

where S is the number of $\phi\rho^0$ signal events, N_ϕ is the number of ϕX background events, N_{ρ^0} is the number of $\rho^0 X$ background events, and B is the number of residual background events, in all nine tiles. The parameter f_i^T is the fraction of events of type T that contributes to tile i. The signal fractions f_i^S are modeled by Monte Carlo (MC) simulation [4], and f_i^ϕ and $f_i^{\rho^0}$ are obtained from the ϕX and $\rho^0 X$ background shapes, which are estimated by fitting the projections of $m_{K^+K^-}$ and $m_{\pi^+\pi^-}$ as described later. The residual background fractions f_i^B are modeled by a linear function that can be expressed as

$$f_i^B = \frac{\Delta x_i \Delta y_i [1 + s_{\rho^0}(x_i - x_5) + s_\phi (y_i - y_5)]}{\sum_{j=1}^{9} \Delta x_j \Delta y_j}, \qquad (2)$$

where Δx_i and Δy_i are the kinematically accessible dimensions of tile i, x_i and y_i are at the center of tile i, and s_{ρ^0} and s_ϕ are slopes obtained from the fits. A similar expression is used for the $\pi^+\pi^-\pi^+\pi^-$ case, where ϕ and ρ^0 are replaced with ρ_f^0 and ρ_b^0.

The background fractions are obtained by mass projection fits which are confined to the central horizontal or central vertical ϕ or ρ^0 resonance band. The effect of neglecting the resonance width outside the central band, checked by smearing the background fractions in the central band into the adjacent tiles using the resonance widths obtained from MC, is found to be negligible. The mass projections in the central bands for $\pi^+\pi^-$ recoiling against a selected ρ^0 or ϕ and for K^+K^- recoiling against a ρ^0 are shown in Fig. 4. For the $\rho^0\pi^+\pi^-$ case we fit the $\pi^+\pi^-$ mass projection to the sum of a ρ^0 component, an $f_2(1270)$ component, and a $\mu^+\mu^-$ background component. The ρ^0 is represented by the product of a P-wave relativistic Breit-Wigner with its width set to the Particle Data Group (PDG) [3] value, a phase space term, and a factor $1/m_{\pi\pi}^2$ due to production via a virtual photon. The $f_2(1270)$ is represented by a D-wave relativistic Breit-Wigner with its mean and width set to the PDG values. The $\mu^+\mu^-$ background shape is obtained from a sample of the related channel $e^+e^- \to \rho^0\mu^+\mu^-$ isolated by requiring two oppositely charged tracks identified as muons. For the $\phi\pi^+\pi^-$ case, we use the same background parameterization in terms of f_2 and $\mu^+\mu^-$, but refit for their normalizations. For the $\rho^0 K^+K^-$ case, we fit the K^+K^- mass projection to the sum of a Breit-Wigner with mean and width fixed to their PDG values for the ϕ signal, and a threshold function $(q^3)/(1+q^3R)$, where q is kaon momentum in the ϕ rest-frame and R is a shape parameter, for background. Assuming the masses of the two pairs to be uncorrelated and excluding the ρ^0 and ϕ signal contributions, the fitted functions are integrated to obtain the tile fractions $f_i^{\rho^0}$, f_i^ϕ, and $f_i^{\rho^0}$.

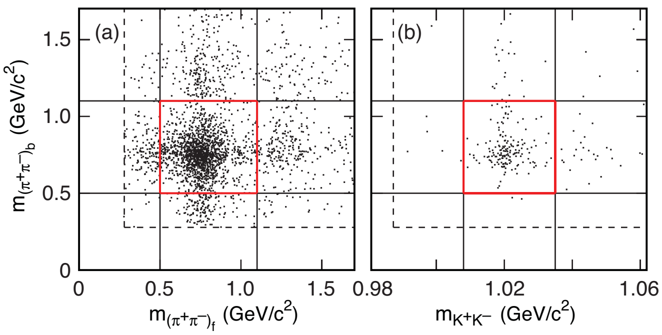

FIG. 3: Scatter plots of the invariant masses of the two oppositely charged pairs in the a) $\pi^+\pi^-\pi^+\pi^-$ and b) $K^+K^-\pi^+\pi^-$ final states. The dashed lines indicate $K^+K^-/\pi^+\pi^-$ thresholds. The solid lines show the nine tiles used in the fit.

The extracted $\rho^0\rho^0$ and $\phi\rho^0$ yields in the signal box are 1243 ± 43 and 147 ± 13 events, to be compared with total of 1508 $\pi^+\pi^-\pi^+\pi^-$ ($\sim$ 18% background) and 163 $K^+K^-\pi^+\pi^-$ ($\sim$ 10% background) events in the signal box, respectively.

To investigate the possibility of $\rho^0\rho^0$ and $\phi\rho^0$ production in $\Upsilon(4S)$ decay, we examine the data recorded at and below the $\Upsilon(4S)$ resonance separately. The yields below the $\Upsilon(4S)$ resonance are 104 ± 14 for $\rho^0\rho^0$ and 14 ± 4 for $\phi\rho^0$, consistent with the expected values of 112 ± 4 and 13 ± 1 obtained by scaling the on-peak yields of 1138 ± 42 and 135 ± 13 by the relative integrated luminosities.

To investigate the production mechanism, we examine the production angle θ^*, defined as the angle between the ρ_f^0 (ϕ) direction and the e^- beam direction in the CM frame. To measure the angular distributions, we subdivide the data into bins of θ^*, and repeat the above fit, with linear background slopes $s_{\rho_f^0}$ and $s_{\rho_b^0}$ (s_{ρ^0} and s_ϕ) fixed to the values from the overall fit. The $|\cos\theta^*|$ distributions after MC efficiency correction are shown in Fig. 5. The measurements are restricted to the fiducial region $|\cos\theta^*| < 0.8$, as the efficiency drops rapidly beyond 0.8. These forward peaking $\cos\theta^*$ distributions are consistent with the TVPA expectation which we find can

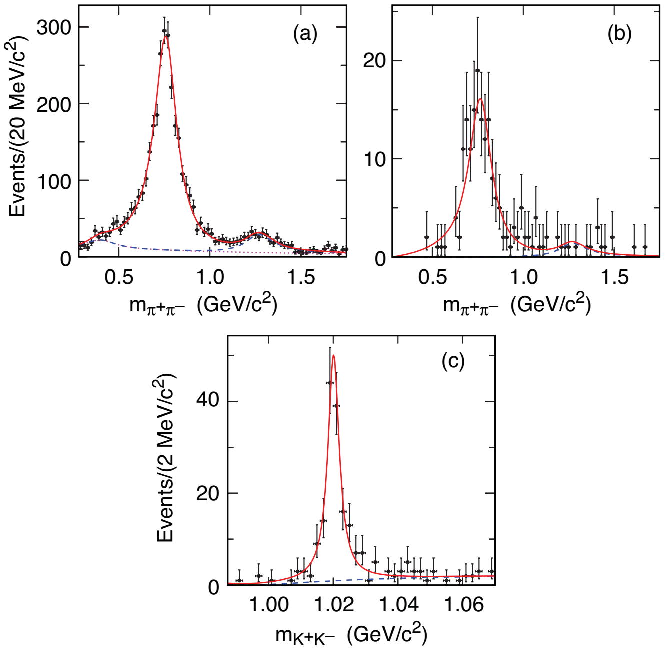

FIG. 4: Mass distribution for a) $\pi^+\pi^-$ pairs in $\rho^0\pi^+\pi^-$ events, b) $\pi^+\pi^-$ pairs in $\phi\pi^+\pi^-$ events, and c) K^+K^- pairs in $\rho^0K^+K^-$ events. The solid curves are the total fit. For the $\pi^+\pi^-$ cases, the dotted curve is the $\mu^+\mu^-$ component, while the sum of $f_2(1270)$ and $\mu^+\mu^-$ contributions are shown as dashed. For the K^+K^- case, the dashed curve represents the threshold function.

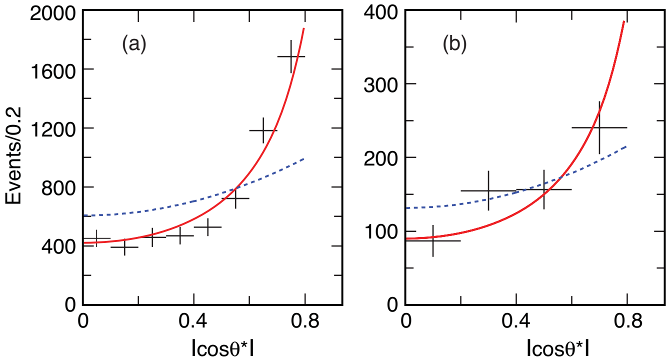

FIG. 5: Production angle distributions, after correction for efficiency, for a) $\rho^0\rho^0$ and b) $\phi\rho^0$. The solid and dashed lines are the normalized $\frac{1+\cos^2\theta^*}{1-\cos^2\theta^*}$ and $1+\cos^2\theta^*$ distributions, respectively.

be approximated by:

$$\frac{d\sigma}{d\cos\theta^*} \propto \frac{1+\cos^2\theta^*}{1-\cos^2\theta^*} \tag{3}$$

in the fiducial region. The TVPA hypothesis gives a χ^2/dof (degrees of freedom) of 11.8/7 ($\rho^0\rho^0$) and 3.5/3 ($\phi\rho^0$). The fits disfavor $1+\cos^2\theta^*$, giving a χ^2/dof of 112/7 for $\rho^0\rho^0$ and 6.3/3 for $\phi\rho^0$.

Other observables are the ϕ (ρ^0) decay helicity angles θ_H, defined as the angle, measured in the ϕ (ρ^0) rest frame, between the positively charged kaon or pion and the flight direction of the ϕ or ρ^0 in the CM frame. The efficiency-corrected distribution of $\cos\theta_H$, obtained using the procedure outline above for θ^*, is shown for the ρ^0 and ϕ candidates in Fig. 6. The solid lines in Fig. 6 are normalized $\sin^2\theta_H$ distributions which give χ^2/dof of 19.3/9 (ρ^0 from $\rho^0\rho^0$), 16.4/9 (ϕ from $\phi\rho^0$), and 3.1/9 (ρ^0 from $\phi\rho^0$). The $\sin^2\theta_H$ distributions indicate that ϕ and ρ^0 are transversely polarized as expected for TVPA. The dihedral angles, the angles between the decay planes of the two vector mesons measured in the CM frame, are consistent with a flat distribution with χ^2/dof of 7.0/9 ($\rho^0\rho^0$) and 10.9/9 ($\phi\rho^0$).

The combined hardware and software trigger efficiencies for signal events in the fiducial region are 99.9% for $\rho^0\rho^0$ and 91.3% for $\phi\rho^0$. The lower efficiency for $\phi\rho^0$ is due to an event shape cut in the software trigger. For the determination of signal cross sections, the MC $\cos\theta^*$ and $\cos\theta_H$ distributions for ϕ and ρ^0 are re-weighted to reproduce the expectation from TVPA. The signal efficiencies in the fiducial region of $|\cos\theta^*|$ <0.8 for $\rho^0\rho^0$ and $\phi\rho^0$ are estimated to be 26.7% and 23.2%, respectively, including corrections to MC simulations of PID, tracking, hardware and software trigger efficiencies. Initial state photon radiation is included in the MC simulation.

Systematic uncertainties due to PID and tracking efficiency are estimated based on measurements from control data samples. The related systematic uncertainties on lepton vetoes are estimated by the difference from not applying the e and μ vetoes on pions. The systematic uncertainty from background subtraction is estimated by varying assumptions about background shapes. We investigated possible feed-down background from related modes with an extra π^0 using various extrapolations from the four-particle mass sidebands. We assume that the final states are fully transversely polarized. The systematic uncertainties are summarized in Table I.

Taking the branching fraction of $\phi \to K^+K^-$ as 49.1% and $\rho^0 \to \pi^+\pi^-$ as 100% [3], and signal mass regions of $0.5 < m_{\rho^0} < 1.1\,\mathrm{GeV}/c^2$ and $1.008 < m_\phi < 1.035\,\mathrm{GeV}/c^2$, we obtain the following results for the TVPA cross sections within $|\cos\theta^*|$ <0.8 near $\sqrt{s} = 10.58\,\mathrm{GeV}$:

$$\begin{aligned} \sigma_{\rm fid}(e^+e^- \to \rho^0\rho^0) &= 20.7 \pm 0.7(\mathrm{stat}) \pm 2.7(\mathrm{syst})\ \mathrm{fb} \\ \sigma_{\rm fid}(e^+e^- \to \phi\rho^0) &= 5.7 \pm 0.5(\mathrm{stat}) \pm 0.8(\mathrm{syst})\ \mathrm{fb}. \end{aligned}$$

The measured cross sections are in good agreement with the calculation from a vector-dominance two-photon exchange model [7].

In summary, we have observed exclusive production of $C = +1$ final states in e^+e^- interactions. The measured C parity configuration, the signal yields in data samples on the $\Upsilon(4S)$ resonance and below, and the production angle distributions support the conclusion that

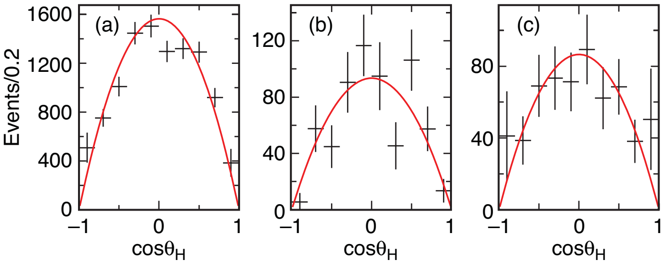

FIG. 6: Decay helicity angle distributions for a) ρ^0 from $\rho^0\rho^0$, b) ϕ from $\phi\rho^0$, c) ρ^0 from $\phi\rho^0$. The solid lines are the normalized $\sin^2\theta_H$ distributions.

TABLE I: Systematic uncertainties on the cross sections for $e^+e^- \to \rho^0\rho^0/\phi\rho^0$.

	$\rho^0\rho^0$	$\phi\rho^0$
Particle Identification	9.6%	10.4%
Background subtraction	7.0%	7.0%
Tracking efficiency	5.0%	5.0%
$\rho^0\rho^0\pi^0, \phi\rho^0\pi^0$ background	1.6%	2.7%
Luminosity	1.2%	1.2%
Total	13.0%	14.0%

the production mechanism is two-virtual-photon annihilation. The Standard Model predictions of the anomalous magnetic moment of the muon and the QED coupling rely on the measurements of low-energy e^+e^- hadronic cross sections, which are assumed to be entirely due to single-photon exchange. We have estimated the effect due to the TVPA processes we have measured, and find it to be small compared with the current precision [1].

We are grateful for the excellent luminosity and machine conditions provided by our PEP-II colleagues, and for the substantial dedicated effort from the computing organizations that support *BABAR*. We wish to thank S. Brodsky, M. Peskin and H. Quinn for helpful discussions. The collaborating institutions wish to thank SLAC for its support and kind hospitality. This work is supported by DOE and NSF (USA), NSERC (Canada), IHEP (China), CEA and CNRS-IN2P3 (France), BMBF and DFG (Germany), INFN (Italy), FOM (The Netherlands), NFR (Norway), MIST (Russia), and PPARC (United Kingdom). Individuals have received support from CONACyT (Mexico), A. P. Sloan Foundation, Research Corporation, and Alexander von Humboldt Foundation.

---

[*] Also at Laboratoire de Physique Corpusculaire, Clermont-Ferrand, France

[†] Also with Università di Perugia, Dipartimento di Fisica, Perugia, Italy

[‡] Also with Università della Basilicata, Potenza, Italy

[1] M. Davier, S. Eidelman, A. Hoecker, Z. Zhang, Eur. Phys. J. C **31**, 503 (2003).
[2] *BABAR* Collaboration, B. Aubert *et al.*, Nucl. Instrum. Methods, Sect. A **479**, 1 (2002).
[3] Particle Data Group, S. Eidelman *et al.*, Phys. Lett. B **592**, 1 (2004).
[4] $e^+e^- \to \rho^0\rho^0/\phi\rho^0$ are generated uniformly over phase space. We use the AFKQED package to simulate the signal processes, including hard and multiple soft initial state radiation, using the methods in [5] and [6].
[5] H. Czyż and J.H. Kühn, Eur. Phys. J. C **18**, 497 (2001).
[6] M. Caffo, H. Czyż, and E. Remiddi, Nuo. Cim. **110A**, 515 (1997); Phys. Lett. B **327**, 369 (1994).
[7] M. Davier, M. Peskin, and A. Snyder, hep-ph/0606155.